

Predissociation of high-lying Rydberg states of molecular iodine via ion-pair states

Alexandr S. Bogomolov, Barbara Grüner, Sergei A. Kochubei, Marcel Mudrich, and Alexey V. Baklanov

Citation: *The Journal of Chemical Physics* **140**, 124311 (2014); doi: 10.1063/1.4869205

View online: <http://dx.doi.org/10.1063/1.4869205>

View Table of Contents: <http://scitation.aip.org/content/aip/journal/jcp/140/12?ver=pdfcov>

Published by the [AIP Publishing](#)

Articles you may be interested in

[Atomic orientation following predissociation of the C 3 g Rydberg state of molecular oxygen](#)

J. Chem. Phys. **138**, 214307 (2013); 10.1063/1.4807761

[Photofragmentations, state interactions, and energetics of Rydberg and ion-pair states: Two-dimensional resonance enhanced multiphoton ionization of HBr via singlet-, triplet-, = 0 and 2 states](#)

J. Chem. Phys. **136**, 214315 (2012); 10.1063/1.4723810

[Predissociation and dissociative ionization of Rydberg states of Xe 2 and the photodissociation of Xe 2 +](#)

J. Chem. Phys. **132**, 124108 (2010); 10.1063/1.3356040

[Proton formation in 2 + 1 resonance enhanced multiphoton excitation of HCl and HBr via \(= 0 \) Rydberg and ion-pair states](#)

J. Chem. Phys. **127**, 124304 (2007); 10.1063/1.2767259

[The field-ionization of near-dissociation ion-pair states of I 2](#)

J. Chem. Phys. **117**, 7117 (2002); 10.1063/1.1503777



Re-register for Table of Content Alerts

Create a profile.



Sign up today!



Predissociation of high-lying Rydberg states of molecular iodine via ion-pair states

Alexandr S. Bogomolov,¹ Barbara Grüner,² Sergei A. Kochubei,³ Marcel Mudrich,² and Alexey V. Baklanov^{1,4}

¹*Institute of Chemical Kinetics and Combustion, Institutskaya Str. 3, Novosibirsk 630090, Russia*

²*Physikalisches Institut, Universität Freiburg, D-79104 Freiburg, Germany*

³*Institute of Semiconductor Physics, ac. Lavrent'ev ave., 13, Novosibirsk 630090, Russia*

⁴*Novosibirsk State University, Pirogova Str. 2, Novosibirsk 630090, Russia*

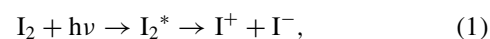
(Received 17 January 2014; accepted 11 March 2014; published online 27 March 2014)

Velocity map imaging of the photofragments arising from two-photon photoexcitation of molecular iodine in the energy range 73 500–74 500 cm⁻¹ covering the bands of high-lying *gerade* Rydberg states [²Π_{1/2}]_c6d;0_g⁺ and [²Π_{1/2}]_c6d;2_g has been applied. The ion signal was dominated by the atomic fragment ion I⁺. Up to 5 dissociation channels yielding I⁺ ions with different kinetic energies were observed when the I₂ molecule was excited within discrete peaks of Rydberg states and their satellites in this region. One of these channels gives rise to images of I⁺ and I⁻ ions with equal kinetic energy indicating predissociation of I₂ via ion-pair states. The contribution of this channel was up to about 50% of the total I⁺ signal. The four other channels correspond to predissociation via lower lying Rydberg states giving rise to excited iodine atoms providing I⁺ ions by subsequent one-photon ionization by the same laser pulse. The ratio of these channels varied from peak to peak in the spectrum but their total ionic signal was always much higher than the signal of (2 + 1) resonance enhanced multi-photon ionization of I₂, which was previously considered to be the origin of ionic signal in this spectral range. The first-tier E0_g⁺ and D'2_g ion-pair states are concluded to be responsible for predissociation of Rydberg states [²Π_{1/2}]_c6d;0_g⁺ and [²Π_{1/2}]_c6d;2_g, respectively. Further predissociation of these ion-pair states via lower lying Rydberg states gives rise to excited I(5s²5p⁴6s¹) atoms responsible for major part of ion signal. The isotropic angular distribution of the photofragment recoil directions observed for all channels indicates that the studied Rydberg states are long-lived compared with the rotational period of the I₂ molecule. © 2014 AIP Publishing LLC. [<http://dx.doi.org/10.1063/1.4869205>]

I. INTRODUCTION

Ion-pair (IP) states usually describe the ground states of highly polar diatomic molecules such as NaCl where the constituent atoms carry large opposite partial charges. The resulting binding potential is then given to good approximation by the Coulomb potential V_C(r) acting between a positive and a negative elementary charge, V_C(r) ~ -e²/r. However, IP states exist for all types of diatomic molecules including covalently bound homonuclear ones. In the latter case they are high-lying in excitation energy and usually strongly coupled to other covalent states due to the high spectral density of these super-excited states. Dissociation of molecules via IP states gives rise to a pair of ions which can be detected with high sensitivity. Therefore, predissociation via IP states provides a window for studying the spectroscopy and dynamics of highly excited electronic states in the coupling regime of covalent and IP states.¹ In the current paper velocity map imaging (VMI) of ions has been applied to study the photodissociation mechanism of super-excited molecular iodine I₂ which is the benchmark system in the field of spectroscopy and dynamics of molecular IP states. The possibility of photodissociation of molecular iodine I₂ via an IP state in

a process,



was first suggested by Mulliken.² Watanabe³ and Myer and Samson⁴ measured the photoionization spectrum of I₂ and interpreted the first photoionization threshold associated with process (1). Morrison *et al.* measured directly the appearance of I⁺ as a product of I₂ photoionization at this first threshold.⁵ Akopyan *et al.* detected simultaneously the formation of both positive I⁺ and negative I⁻ ions with identical spectral profiles of their generation within the first photoionization band.⁶ Akopyan *et al.*⁶ assumed the IP I⁺ + I⁻ to arise from predissociation of Rydberg states. Kvaran *et al.* recorded the spectral function of the appearance of both I⁺ and I⁻ ions after one-photon excitation of I₂ with radiation tuned in the region 120–140 nm.⁷ Higher spectral resolution allowed the authors of Ref. 7 to reveal the structure of the band responsible for IP photogeneration. This structure was attributed to the excitation of vibrational levels of several Rydberg series. Similar studies but with higher spectral resolution were carried out by Lawley *et al.*⁸ These authors observed a dense spectral structure of transitions giving rise to free ion

pairs $I^+ + I^-$. This structure closely follows the one-photon absorption spectrum. Several Rydberg series were identified. Direct absorption to the continuum of IP states was found to be negligible. All Rydberg states were concluded to be efficient doorway states to IP production.

Multiphoton schemes giving rise to excitation of IP states in I_2 have also been used. Earlier results on the multiphoton spectroscopy of high-lying electronic states involving IP states in I_2 and other halogen and interhalogen molecules were reviewed by Brand and Hoy.⁹ The energy region near the first IP dissociation threshold was probed by Ridley *et al.* using a three-color multiphoton scheme for excitation and a pulsed electric field for dissociation of subthreshold IP states.¹⁰ They concluded that direct multiphoton excitation to the highly vibrationally excited levels of dissociating IP states can be ruled out. The doorway states are suggested to be Rydberg states or second-tier IP states or mixed states created by the coupling of the two types. The energy region corresponding to excitation above as well as below threshold for free ion pair $I^+ + I^-$ formation has also been investigated by Donovan *et al.*¹¹ who studied the $(2 + 1)$ resonance enhanced multi-photon ionization (REMPI) spectrum of I_2 . The latter was found to consist of a discrete part and a continuous background. The observed discrete structure was assigned to several series of *gerade* Rydberg states. The source of the continuous background remained uncertain. In that paper the total ionic signal from the ionization of gaseous I_2 at ambient temperature was measured. Therefore, it was not possible to draw any conclusions on the contribution of IP production.

In the current paper we apply velocity map imaging of cationic and anionic photofragments to establish the nature of the dissociation channels which are active when I_2 molecules are two-photon excited into the Rydberg states which lie above the dissociation limit of the first-tier IP states.

II. EXPERIMENT

In our experiment, cold I_2 molecules were generated in a pulsed molecular beam apparatus. The supersonic beam with duration of 100 μ s was generated by a home-made electrodynamic valve. To deliver I_2 vapor into the valve volume the helium carrier gas flowed through a vessel filled with beads of iodine crystals at room temperature, providing I_2 vapor pressure of about 0.2 Torr. The premixed gas expanded into the vacuum chamber through a nozzle with an orifice diameter of 0.27 mm. The backing pressure was held constant at 1 atm. The central part of the gas jet passed through the 2.5 mm skimmer mounted 60 mm downstream and entered the region of a homogeneous electric field created by the electrodes of a time-of-flight mass-spectrometer (TOFMS). The molecular beam was directed perpendicular to the TOF-MS axis. In this region the pulsed UV laser radiation crossed the molecular beam at a right angle. This tunable UV radiation (1 mJ per pulse) was produced as a second harmonic of a pulsed dye laser (Coumarine 153) pumped by an excimer XeCl laser (308 nm, 100 mJ, 15 ns). The dye laser wavelength was measured by wavelength meter (WS-6 by Angstrom Co.). The UV radiation tuned around 270 nm was polarized along the

molecular beam axis and perpendicularly to the TOFMS axis. The radiation was focused by a lens with a focal length of 15 cm. The ions were detected by a microchannel plate (MCP) detector (F2225-21P MCP assembly by Hamamatsu).

The arrangement used for velocity map imaging of I^+ and I^- ions was similar to that used by Eppink and Parker¹² with an off-axis arrangement of the pulsed valve. A three-electrode electrostatic lens with two open electrodes with holes 16 mm in diameter was used for extracting the ions. The MCP was used as a two-dimensional ion detector. The 2D images on the phosphor screen were recorded by a CCD camera (Videoscanner 285/O-2001) with a $f = 2.5$ cm objective and stored in a PC. The images which were averaged over several thousand shots were inverted using the pBasex method.¹³

III. RESULTS AND DISCUSSION

A. Photoionization spectrum of cold I_2

The mass-spectra of ions generated via excitation within the features of the $(2 + 1)$ REMPI spectrum of I_2 from the paper by Donovan *et al.*¹¹ in the investigated wavelength region contained two peaks with $m/z = 127$ and 254 corresponding to I^+ and I_2^+ ions where the latter signal is lower than the one of I^+ by two orders of magnitude. The spectral dependence of the I^+ amplitude was recorded in the region from 268.5 nm to 272.1 nm corresponding to the two-photon excitation energy within the wave number interval 73 500–74 500 cm^{-1} . In this range Donovan *et al.*¹¹ had observed two well pronounced series of bands assigned to transitions into states of the $[^2\Pi_{1/2}]_c 8s; 0_g$ and $[^2\Pi_{1/2}]_c 8s; 1_g$ Rydberg series as well as a number of REMPI lines of the I atom. Later, polarization studies as well as rotational contour analysis have been carried out by the same group for $(2 + 1)$ REMPI spectrum of the bromine Br_2 molecule where similar Rydberg band series were assigned to the $6d$ state.¹⁴ The similarity of the REMPI spectra of the halogens Cl_2 , Br_2 , and I_2 which were referenced to more accurately determined values of ionization potentials of the I_2 molecule indicate that these series actually are $[^2\Pi_{1/2}]_c 6d; 2_g$ and $[^2\Pi_{1/2}]_c 6d; 0_g^+$ states, respectively.¹⁵ Figure 1 shows spectral fragments of the I^+ photoionization spectrum for regions corresponding to these Rydberg bands as well as to several $(2 + 1)$ REMPI lines of the I atom. For comparison the spectrum obtained for I_2 in gas phase at ambient temperature¹¹ is also presented. Our data obtained with cold I_2 molecules generated in a pulsed molecular beam provide narrower lines. These narrow lines define more precisely the positions of the vibronic bands (v' , v'') of these series. Here, v' denotes the vibrational quantum number of the upper state and v'' that of the lower state of the transition. In our spectrum we see strong lines coinciding in position with the values for (0,0) bands assigned by Donovan *et al.*¹¹ The spectrum of cold I_2 in Figure 1 also contains lines shifted from the (0,0) lines to the red by 213 cm^{-1} which corresponds to the gap between ground and first excited vibrational levels of I_2 molecule in the ground electronic state. Thus, we attribute these lines to hot bands (0,1). Rather limited vibrational cooling of I_2 at comparable supersonic jet expansion conditions was observed earlier by Chestakov *et al.* who measured a vibrational

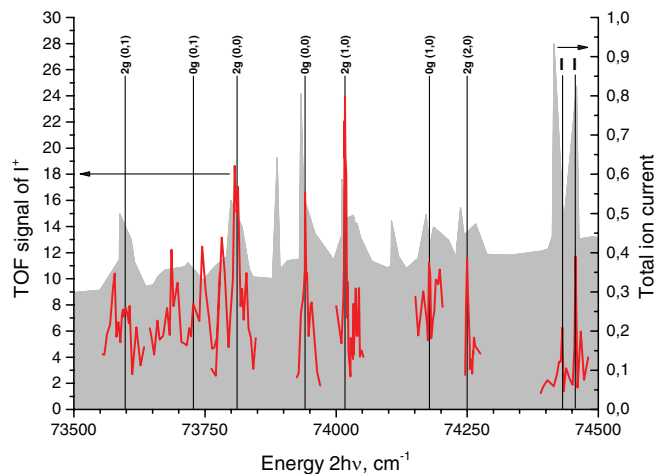


FIG. 1. Red lines show the excitation spectra (left axis) for I^+ signal in the time-of-flight mass-spectrum provided by excitation of I_2 . Gray background corresponds to REMPI spectra (right axis) measured in gaseous I_2 at room temperature by Donovan *et al.*¹¹ In the assignment 0_g and 2_g mean excitation to the states of Rydberg $[^2\Pi_{1/2}]_c6d;0_g^+$ and $[^2\Pi_{1/2}]_c6d;2_g$ series, respectively.

temperature of I_2 in molecular beam of 240 ± 10 K.¹⁶ Thus, it is plausible that hot bands contribute under the conditions of our pulsed molecular beam. The assignment of these bands to hot transitions will be discussed later when taking into account the velocity map imaging data. Other vibronic bands (1,0) and (2,0) were assigned to intense lines closest to the positions suggested by Donovan *et al.*¹¹ This assignment is shown in Figure 1. Table I lists the positions of the peaks from Ref. 11 with the assignment discussed above as well as our data. At the position of the (2,0) band¹¹ from the series assigned to be $[^2\Pi_{1/2}]_c6d;0_g^+$ the very intense contribution of the (2 + 1) REMPI lines of $I(^2P_{1/2})$ atoms (see below) prevented us from detecting any other contributions which could belong to Rydberg series. Therefore, we refrain from specifying a number for this transition in Table I. The other lines in the spectrum of cold I_2 in Fig. 1 could belong to the other Rydberg series or to nearby lying states of the second-tier IP vibrational manifold¹⁰ as well as to REMPI lines of the I atom (see below).

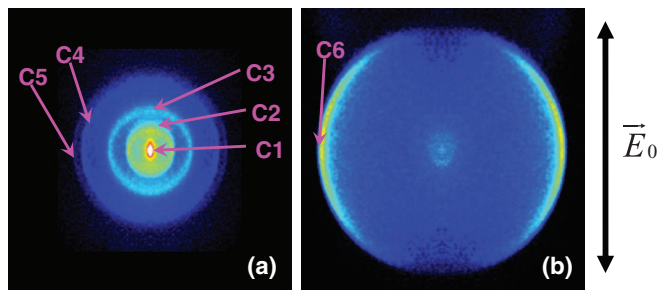


FIG. 2. Velocity map images of I^+ ions resulting from photoexcitation of I_2 molecules: (a) Excitation at 270.486 nm ($2h\nu = 73\,941\text{ cm}^{-1}$) corresponding to the (0,0) band of the Rydberg $[^2\Pi_{1/2}]_c6d;0_g^+$ series; (b) excitation at 268 731 nm, corresponding to the (2 + 1) REMPI line of $I(^2P_{1/2})$ (see text). The double-headed arrow indicates the direction of the linear polarization.

B. Velocity map images and their interpretation

At the wavelengths corresponding to all the peaks in the spectrum of cold I_2 in Figure 1 we recorded velocity map images of I^+ ions. The observed images resembled either one of the two typical images presented in Figure 2. The ring structures in the image shown in Figure 2(a) indicates that five dissociation channels C1–C5 are active which give rise to I^+ ions with different kinetic energies. All these channels are almost isotropic in terms of the angular distribution of the I^+ recoil direction (anisotropy parameter $\beta \approx 0$). Abel inversion of the images and angular integration provides the distribution of I^+ ions as a function of kinetic energy. The measured kinetic energy of I^+ ions multiplied by factor 2 gives the Total Kinetic Energy Release (TKER) in the dissociation via the channels under consideration. For assigning the channels with experimentally measured values of TKER we calculate the energy of the dissociation limit for each of the channels observed. The energy value

$$E^* = 2h\nu - D_0^0(I - I) - \text{TKER} \quad (2)$$

just corresponds to the potential energy of the photofragments counted from zero energy as given by two free iodine atoms in the ground state $I(^2P_{3/2})$. The results of the conversion of the images obtained at several excitation wavelengths are presented in Figure 3. All TKER spectra display maxima at identical positions, E^*_{1-5} labeled C1–C5 except for the one at

TABLE I. Positions of the lines corresponding to the Rydberg series in the two-photon absorption spectrum of I_2 with the assignment of vibrational states involved in the transition from Ref. 11

Rydberg series	Vibrational states involved in the transition (v', v'')	Line positions from Ref. 11, cm^{-1}	Line positions (this work), cm^{-1}
$[^2\Pi_{1/2}]_c6d;0_g^+(v', v'')$	(0,1) ^a	73 720	73 728
	(0,0)	73 941	73 941
	(1,0)	74 178	74 178
	(2,0)	74 417	... ^b
	(0,1) ^a	73 595	73 598
$[^2\Pi_{1/2}]_c6d;2_g(v', v'')$	(0,0)	73 811 ^c	73 811
	(1,0)	74 034	74 017
	(2,0)	74 263	74 250

^aThis assignment is discussed in Sec. III B.

^bThis line is masked by strong REMPI (2+1) line of $I(^2P_{1/2})$ atom.

^cIn Table 2 of Ref. 11 this number is given with a misprint.

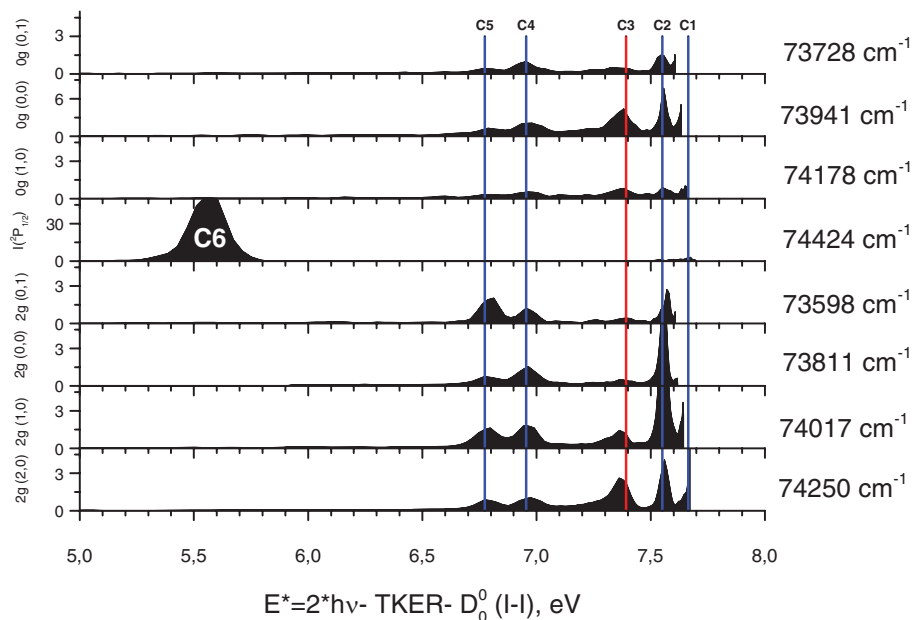
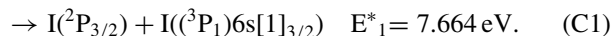
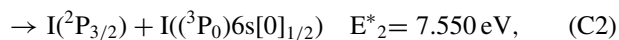
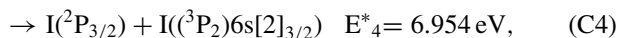
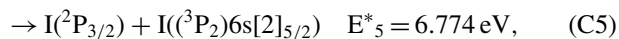
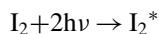
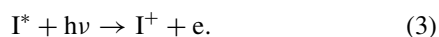


FIG. 3. The results of the conversion of experimentally measured velocity map images of I^+ resulting from photoexcitation of I_2 at several wavelengths. The two-photon energies for UV-radiation used are given on the right side of the figure. On the left the assignment (see text) and ordinate axes showing the amplitudes of ionic signal are given. The vertical lines show the peak positions corresponding to channels giving rise to the free ion pair $I^+ + I^-$ (C3) and to the pair of atoms $I(^2P_{3/2}) + I^*$ (C1, C2, C4, and C5), where I^* is the iodine atom in an excited state (see text). Designations 0_g and 2_g on the left mean excitation to the states of Rydberg $[^2\Pi_{1/2}]_c6d;0_g^+$ and $[^2\Pi_{1/2}]_c6d;2_g$ series, respectively.

$2h\nu = 74424 \text{ cm}^{-1}$ which features only one dominant peak (C6) to be discussed later. Peaks 1–5 can be explained by two-photon excitation of I_2 followed by dissociation via the following channels:

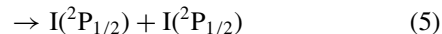
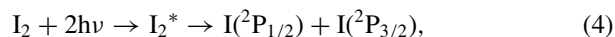


The threshold values E_{1-5}^* for channels C1, C2, C4, and C5 are calculated using energy values for excited states of the iodine atom from the NIST database¹⁵ and are depicted as vertical lines in Figure 3. For channel C3, E_3^* is calculated using the value of the ionization potential¹⁷ of I, $E_{IP,I} = 84295 \text{ cm}^{-1} = 10.45 \text{ eV}$, and the electron affinity¹⁸ of I $E_{EA,I} = 24673 \text{ cm}^{-1} = 3.06 \text{ eV}$. In the channel C3 the ion I^+ appears directly. In other channels it appears due to one-photon photoionization by the same laser pulse according to



At the wavelengths used, the photon energy $h\nu \approx 4.6 \text{ eV}$ is sufficient for one-photon ionization of excited states of

atomic iodine I^* with energy higher than about 5.85 eV. Excited states I^* arising in channels C1, C2, C4, and C5 fit this condition. These channels correspond to four excited states $I(^3P_2)6s[2]_{5/2}$, $I(^3P_2)6s[2]_{3/2}$, $I(^3P_0)6s[0]_{1/2}$, and $I(^3P_1)6s[1]_{3/2}$ as shown in Figure 4. The maximum energy of two photons $2h\nu = 9.21 \text{ eV}$ in our experiments can provide iodine atoms with excitation energy up to $2h\nu - D_0(I - I) = 7.68 \text{ eV}$. Five excited states of iodine atom are energetically accessible at this excitation level involving the lowest excited state $I(5s^25p^5(^2P_{1/2}))$ and four higher lying states of electronic configuration $I(5s^25p^46s^1)$. We see all these four $I(5s^25p^46s^1)$ states arising in C1, C2, C4, and C5 channels which become visible in velocity map imaging due to photoionization (3). The lowest excited state $I(^2P_{1/2})$ can only be ionized by the absorption of three or more photons, which we observe as channel C6. However, conceivable pathways leading to the dissociation into $I(^2P_{1/2})$ atoms via two-photon excitation according to the channels



were not observed (see comments in Sec. III B). All observed channels are shown in Figure 4. The appearance of excited states of I atoms was previously observed by Hiraya *et al.*¹⁹ who studied the fluorescence excitation spectrum of I_2 . These authors studied one-photon excitation of I_2 using tunable synchrotron VUV radiation and recorded the fluorescence of two excited states of the I atom ($I(^3P_0)6s[0]_{1/2}$ and $I(^3P_1)6s[1]_{3/2}$) with excitation thresholds just corresponding to the appearance thresholds for these states. Neutral photodissociation channels giving rise to high- n Rydberg I atoms contribute to the dissociation of superexcited Rydberg states

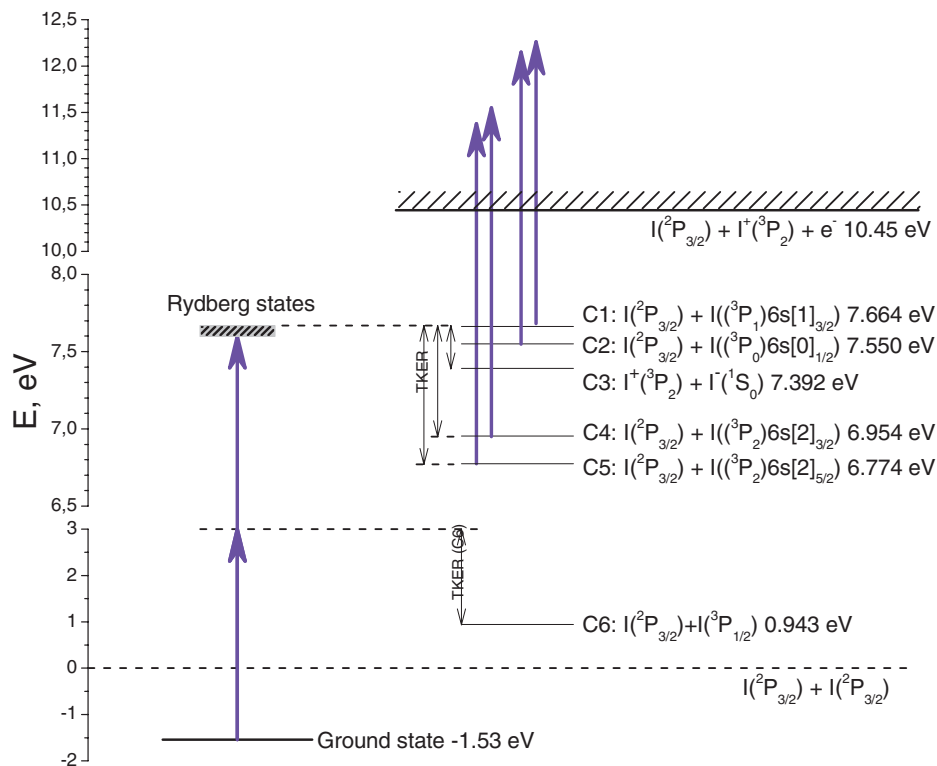
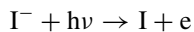


FIG. 4. Scheme of the processes proceeding after two-photon excitation of the I_2 Rydberg states within the spectral region under study.

of I_2 even when the level of excitation is much higher than the I_2 photoionization limit.²⁰

In contrast to the channels discussed so far, C3 is interpreted as the dissociation into a free ion pair $I^+ + I^-$ following two-photon excitation. This interpretation is confirmed by reversing the voltages of our VMI spectrometer and by recording an ion image of the negative ion I^- (Figure 5).

For anions only one channel is observed which gives rise to I^- with similar TKER as C3 for I^+ ions. The very low level of signal in the I^- image can be understood when taking into account the possibility of electron photodetachment



by the same laser pulse. The energy of one photon $h\nu \approx 4.6$ eV exceeds the electron affinity of atomic iodine $E_{ea,I}$

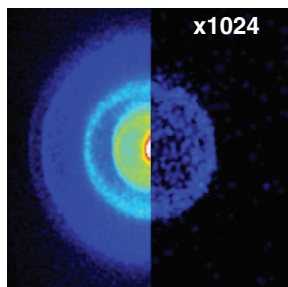


FIG. 5. Velocity map images of I^+ (left part) and I^- ions (right part, enhanced by factor 1024) resulting from photoexcitation of molecular iodine at 270.486 nm ($2h\nu = 73\,941\text{ cm}^{-1}$), corresponding to the (0,0)-band of the $[^2\Pi_{1/2}]_c6d;0_g^+$ Rydberg series.

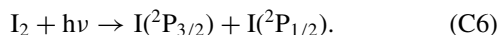
≈ 3.06 eV. The energy fluence in the focus of the laser beam is estimated to be $\geq 10\text{ J/cm}^2 \approx 10^{19}$ photons/cm². Under these conditions we expect an attenuation of the signal by about a factor 10^{-3} provided the cross-section of electron photodetachment from I^- amounts to about 10^{-18} cm^2 or higher at the wavelength used, which appears quite realistic. A similar process involving the formation of ion pairs and highly excited electronic states of atomic fragments followed by photodetachment of electron from the anionic fragment was observed when exciting high lying Rydberg states in molecular oxygen.²¹

Here it is worth emphasizing that velocity map imaging turns out to be an efficient method for detecting simultaneously ionic and neutral channels that contribute to the photodissociation of molecular Rydberg states. Moreover, it allows one to estimate the ratio of the photodissociation channels quantitatively. Typical values for the cross-sections of one-photon ionization of excited atoms fall into the range 10^{-17} to 10^{-18} cm^2 .²² In our focusing conditions with a photon fluence of $\geq 10^{19}\text{ cm}^{-2}$ one-photon ionization (3) must be saturated. So the integrals of the peaks in the images of I^+ presented in Figure 2 should correspond to the absolute yields of corresponding ionic or neutral photodissociation channels. The contribution of ion-pair channel C3 in total ionic signal varied with excitation wavelength (see Fig. 3). The upper limit of this contribution was about 50% whereas the lowest contribution was less than 10% of the total I^+ signal. The rest of the ionic signal with a contribution up to more than 90% was provided by neutral photodissociation channels C1, C2, C4, and C5 giving rise to Rydberg I atoms. These numbers

correspond to the contributions of ion-pair and neutral channels in the photodissociation of I_2 Rydberg states in the spectral range under study.

On the basis of these results we can expect that the ionic signal measured by REMPI mediated by resonant excitation of molecular Rydberg states is very often provided by “indirect REMPI” due to dissociation of Rydberg states via neutral channels followed by one-photon photoionization of product Rydberg atoms. This conclusion holds for I_2 and can hold for other molecules as well.

In Figure 2(b) we see a much more intense image with one dominating and highly anisotropic ring (anisotropy parameter $\beta = -1.05 \pm 0.07$). The result of Abel inverting this image is shown in Fig. 3 as well (channel C6). Based on the extracted TKER value 2.14 eV we attribute this channel to one-photon photodissociation of I_2 :



This image is generated by iodine atoms in the first excited state $I(^2P_{1/2})$ ionized via a (2 + 1) REMPI scheme. The sum of the two-photon energy $2h\nu \approx 74424 \text{ cm}^{-1}$ and the energy 7603 cm^{-1} of the state $I(^2P_{1/2})$ is close within a few wavenumbers to the energy of a number of states of the I atom¹⁵ providing resonances for two-photon absorption by $I(^2P_{1/2})$. One-photon photodissociation of I_2 proceeding via channel C6 with excitation at the nearby wavelengths 266.2 nm was observed by Clear and Wilson.²³ These authors reported negative angular anisotropy of this transition and assigned the dissociative state to the $1_u(^3\Sigma^+)$ state. Velocity map images of I atoms similar to that given in Figure 2(b) and corresponding to channel C6 were observed previously by Vidma *et al.*²⁴ when molecular I_2 was excited at the nearby wavelength 250 nm.

The image of the $I(^2P_{1/2})$ atom displayed in Figure 2(b) shows only the central part of image involving the ring of C6 channel. Outside this part we did not see any contributions. In particular, we point out that we did not find any indication for the formation of $I(^2P_{1/2})$ atoms with translational energy corresponding to the dissociation of two-photon excited I_2 molecules via processes (4) and (5) mentioned above.

In Figure 6 the spectral dependence of the yields of channels C2–C5 is shown for the excitation in the spectral vicinity of the transition to the Rydberg state $[^2\Pi_{1/2}]_c6d;0_g^+(0,0)$. In this spectral region the two-photon excitation energy is less than the threshold value for the appearance of channel C1. Similar spectral behavior of all the contributions within one peak indicates its homogeneous nature. The ratio of the yields of channels C2–C5 in turn varies from peak to peak, i.e., this ratio is specific for each state excited. These peaks can be due to the interaction of the Rydberg states under study with nearby discrete levels of the second-tier IP $f0_g^+$ vibrational manifold. The spacing between two weaker lines in Figure 6 is about 25 cm^{-1} . This number should be compared with the estimated average interval between the vibrational levels of the second-tier IP state $f0_g^+$ at the energy level of the Rydberg state (73941 cm^{-1}). This total energy corresponds to about 27000 cm^{-1} of vibrational energy in $f0_g^+$ state. To estimate this average interval the density of vibrational states of the $f0_g^+$ vibrational manifold at this energy level is esti-

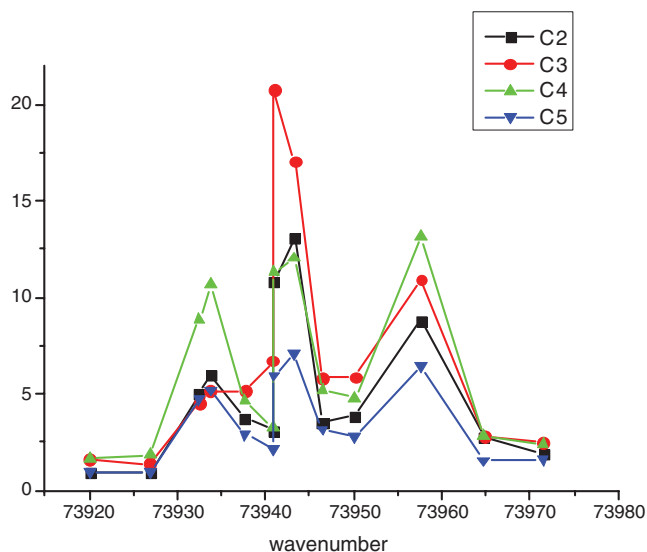


FIG. 6. The spectral dependence of the yields of channels C2–C5 in the vicinity of Rydberg transition $[^2\Pi_{1/2}]_c6d;0_g^+(0,0)$.

ated. We approximate the shape of the $f0_g^+$ potential curve by a Morse potential with parameters $T_e = 47025 \text{ cm}^{-1}$, $D_e = 31590 \text{ cm}^{-1}$, and $\omega_e = 104.2 \text{ cm}^{-1}$ given in Ref. 9. This rough estimate gives an interval of 40 cm^{-1} which is comparable with the spacing between the two weaker components of the line triplet in Figure 6.

The results of velocity map imaging allow us to verify the assignment of the bands as hot bands in the Rydberg series presented in Table I. The lines with the two-photon energies 73728 and 73598 cm^{-1} correspond to the hot bands (0,1) for the series $[^2\Pi_{1/2}]_c6d;0_g^+$ and $[^2\Pi_{1/2}]_c6d;2_g$, respectively. Transitions (0,1) and (0,0) of one Rydberg series have the same final state. This state is the initial one for the further dynamics in the excited molecule. The same initial state should provide the same intensity ratio of the channels in the images resulting from excitation within these two lines. However, when comparing the KER spectra in Fig. 3 measured at 73728 and at 73941 cm^{-1} we see a clear difference in the relative contribution of the C1 and C3 channels. The same is true for the images at 73598 and 73811 cm^{-1} where the contribution of the channels C4 and C5 vary. These results may indicate that the lines assigned earlier to hot transitions need to be reassigned. We can assume these lines to be due to transitions to the levels of the second-tier IP vibrational manifold.

C. Mechanism of predissociation from two-photon excited Rydberg states of I_2

To draw further conclusions on the nature of the observed channels let us consider the scheme of potential energy curves for the states involved which is presented in Figure 7. As we have established in this work, one-photon excitation populates the repulsive state $C1_u$ which then dissociates via process C6. The repulsive state $C1_u$ is presented in Figure 7 as a Morse potential $E = T_e + D_e \cdot (1 - \exp(-a \cdot (R - R_e)))^2$ with parameters obtained on the basis of *ab initio* calculations by de Jong *et al.*²⁵ The value of the slope of the potential a was modified

observed widths of lines do not contradict upper conclusion on time-scale of predissociation.

The results obtained above allow us to return to the interpretation of the ionic signal in the experiments by Donovan *et al.*¹¹ assigned to (2 + 1) REMPI of I₂. Our experiments show that the contribution of I₂⁺ to the total ionic signal in the energy region 73 500–74 500 cm⁻¹ under study is negligible as compared with the I⁺ contribution. In turn, I⁺ ions are produced by two different types of processes both starting with the predissociation of two-photon excited Rydberg states of I₂ via IP states. The first type corresponds to predissociation giving rise to the ion pair I⁺ + I⁻ directly with further photodetachment of the electron from the anion I⁻ by the same laser pulse. This contribution becomes relevant at excitation energies above the threshold for IP formation (71 955 cm⁻¹). The second contribution is provided by further predissociation of the IP state via lower-lying Rydberg states followed by the formation of excited I atoms. These I atoms are photoionized by one photon of the same laser pulse. This last contribution is also three-photon in nature akin to (2 + 1) REMPI but differs from direct photoionization of I₂ molecules. This mechanism should be active for two-photon energies exceeding about 67 055 cm⁻¹ which is sufficient for forming I atoms in the second excited state I((³P₂)6s[2]_{5/2}). These processes of sequential excitation, dissociation, and ionization can compete with and even dominate over the direct REMPI process in other molecules as well.

IV. CONCLUSIONS

Velocity map imaging has been applied to study the mechanism of predissociation of two-photon excited I₂ molecules from Rydberg states of 6*d*-series in the energy region above the dissociation limit of the first-tier ion-pair states.

Mass spectra show that 99% of the total ions are due to I⁺. The two-photon action spectrum of I⁺ contains lines of the [²Π_{1/2}]_c6*d*;0_g⁺ and [²Π_{1/2}]_c6*d*;2_g Rydberg series accompanied by some weaker satellite bands which we interpret to be due to the interaction of Rydberg states with nearby lying vibrational levels of the second-tier ion-pair states. All photogenerated I⁺ ions are found to appear via six different channels identified according to the translational energy values of the photofragments. Five of these channels correspond to photodissociation of the two-photon excited I₂ molecules. One of them is found to give rise to the ion pair I⁺ + I⁻ with identical velocity map images for the I⁺ and I⁻ ions. Four other channels correspond to the formation of excited I atoms in the Rydberg 6*s* states which are energetically accessible. These Rydberg states of the I atom give rise to I⁺ ions via one-photon ionization by radiation of the same laser pulse. The intensity ratio of contributions of these ion-pair and neutral channels depend on the state excited. The contribution of the ion-pair channel varied from about 50% to less than 10% of the total photodissociation yield with the rest being neutral channels. For all these five channels the angular distribution of the recoil directions of the photofragments was found to be isotropic. This indicates that Rydberg states under study are long-lived compared with the rotational period

of the I₂ molecule. Photodissociation is concluded to proceed as predissociation of the two-photon excited Rydberg states via the first-tier ion-pair state. The states of [²Π_{1/2}]_c6*d*;0_g⁺ and [²Π_{1/2}]_c6*d*;2_g Rydberg series are assumed to predissociate via E0_g⁺ and D'2_g ion pair states, respectively. Neutral channels are likely to proceed via avoided crossing of IP states with lower lying molecular Rydberg states giving rise to a pair of neutral I atoms. One I atom appears in the ground ²P_{3/2} state and the other one in the excited I(5*s*²5*p*⁴6*s*¹) state which is then photoionized by the same laser pulse with efficiency close to unity.

The results obtained demonstrate that velocity map imaging allows one to detect, identify, and estimate quantitative contributions of dissociation channels giving rise to ions and to highly excited neutrals simultaneously. This capability makes velocity map imaging very efficient for the study of the photophysics and photochemistry of high-lying molecular states.

The results obtained allow us to conclude that the ionic signal measured in resonance-enhanced multiphoton ionization spectroscopy can often be indirect REMPI in nature. This especially applies to REMPI mediated by resonant excitation of molecular Rydberg states where photodissociation of Rydberg states via neutral channels followed by one-photon ionization of the appearing highly excited atoms by the same laser pulse can provide a major fraction of the ionic signal. This signal is still resonance-enhanced but not due to multiphoton ionization of the precursor species as it is usually supposed. This conclusion is definitely applicable for REMPI of I₂ mediated by two-photon resonances with Rydberg states in the spectral region studied in this work and may apply to other molecules as well.

ACKNOWLEDGMENTS

Financial support for this work by the Deutsche Forschungsgemeinschaft (Grant No. MU 2347/7-1) and by the Russian Foundation for Basic Research (Grant Nos. 13-03-91333 and 12-03-00170) is gratefully acknowledged. The authors thank the reviewer of the Journal of Chemical Physics for very useful recommendations.

- ¹A. G. Suits and J. W. Hepburn, *Annu. Rev. Phys. Chem.* **57**, 431 (2006).
- ²R. S. Mulliken, *Phys. Rev.* **46**, 549 (1934).
- ³K. Watanabe, *J. Chem. Phys.* **26**, 542 (1957).
- ⁴J. A. Myer and J. A. R. Samson, *J. Chem. Phys.* **52**, 716 (1970).
- ⁵J. D. Morrison, H. Hurlzeler, M. G. Inghram, and H. E. Stanton, *J. Chem. Phys.* **33**, 821 (1960).
- ⁶M. E. Akopyan, F. I. Vilesov, and Yu. L. Sergeev, *Opt. Spectrosc.* **35**, 472 (1973).
- ⁷A. Kvaran, A. J. Yench, D. K. Kela, R. J. Donovan, and A. Hopkirk, *Chem. Phys. Lett.* **179**, 263 (1991).
- ⁸K. P. Lawley, A. C. Flexen, R. R. J. Maier, A. Manck, T. Ridley, R. J. Donovan, *Phys. Chem. Chem. Phys.* **4**, 1412 (2002).
- ⁹J. C. D. Brand and A. R. Hoy, *Appl. Spectrosc. Rev.* **23**, 285 (1987).
- ¹⁰T. Ridley, M. de Vries, K. P. Lawley, S. Wang, and R. J. Donovan, *J. Chem. Phys.* **117**, 7117 (2002).
- ¹¹R. J. Donovan, R. V. Flood, K. P. Lawley, A. J. Yench, and T. Ridley, *Chem. Phys.* **164**, 439 (1992).
- ¹²A. T. J. B. Eppink and D. H. Parker, *Rev. Sci. Instrum.* **68**, 3477 (1997).
- ¹³G. A. Garcia, L. Nahon, and I. Powis, *Rev. Sci. Instrum.* **75**, 4989 (2004).
- ¹⁴R. J. Donovan, A. C. Flexen, K. P. Lawley, and T. Ridley, *Chem. Phys.* **226**, 217 (1998).

- ¹⁵T. Ridley, D. A. Beattie, M. C. R. Cockett, K. P. Lawley, and R. J. Donovan, *Phys. Chem. Chem. Phys.* **4**, 1398 (2002).
- ¹⁶D. A. Chestakov, D. H. Parker, K. V. Vidma, and T. P. Rakitzis, *J. Chem. Phys.* **124**, 024315 (2006).
- ¹⁷A. Kramida, Yu. Ralchenko, J. Reader, and NIST ASD Team (2012), NIST Atomic Spectra Database version 5.0, available at <http://physics.nist.gov/asd> [11 June 2013], National Institute of Standards and Technology, Gaithersburg, MD.
- ¹⁸D. Hanstorp and M. Gustafsson, *J. Phys. B* **25**, 1773 (1992).
- ¹⁹A. Hiraya, K. Shobatake, R. J. Donovan, and A. Hopkirk, *J. Chem. Phys.* **88**, 52 (1988).
- ²⁰P. O’Keeffe, D. Stranges, and P. L. Houston, *J. Chem. Phys.* **127**, 144309 (2007).
- ²¹A. V. Baklanov, L. M. C. Janssen, D. H. Parker, L. Poisson, B. Soep, J.-M. Mestdagh, and O. Gobert, *J. Chem. Phys.* **129**, 214306 (2008).
- ²²V. S. Letokhov, *Laser Photoionization Spectroscopy* (Academic Press, New York, 1987), 353 pp.
- ²³R. D. Clear and K. R. Wilson, *J. Mol. Spectrosc.* **47**, 39 (1973).
- ²⁴K. V. Vidma, A. V. Baklanov, E. B. Khvorostov, V. N. Ishchenko, S. A. Kochubei, A. T. J. B. Eppink, D. A. Chestakov, and D. H. Parker, *J. Chem. Phys.* **122**, 204301 (2005).
- ²⁵W. A. de Jong, L. Visscher, and W. C. Nieuwpoort, *J. Chem. Phys.* **107**, 9046 (1997).
- ²⁶M. Tamres, W. K. Duerksen, and J. M. Goodenow, *J. Phys. Chem.* **72**, 966 (1968).
- ²⁷M. C. R. Cockett, J. G. Goode, K. P. Lawley, and R. J. Donovan, *J. Chem. Phys.* **102**, 5226 (1995).
- ²⁸J. C. D. Brand, A. K. Kalukar, and A. B. Yamashita, *Opt. Commun.* **39**, 235 (1981).
- ²⁹A. Kalmos, A. Valdes, and R. Prosimiti, *J. Phys. Chem. A* **116**, 2366 (2012).
- ³⁰P. J. Wilson, T. Ridley, K. P. Lawley, and R. J. Donovan, *Chem. Phys.* **182**, 325 (1994).
- ³¹R. N. Dixon, *J. Chem. Phys.* **122**, 194302 (2005).